Applied Surface Science 411 (2017) 1–10

Contents lists available at ScienceDirect

Applied Surface Science

journal homepage: www.elsevier.com/locate/apsusc

Full Length Article

Ga-doped and antisite double defects enhance the sensitivity of boron nitride nanotubes towards Soman and Chlorosoman

Masoud Bezi Javan[a], Alireza Soltani[b,c,*], A.S. Ghasemi[d], E.Tazikeh Lemeski[e], Niloofar Gholami[c], Hanzaleh Balakheyli[b]

[a] Physics Department, Faculty of Sciences, Golestan University, Gorgan, Iran
[b] Golestan Rheumatology Research Center, Golestan University of Medical Science, Gorgan, Iran
[c] Young Researchers and Elite Club, Gorgan Branch, Islamic Azad University, Gorgan, Iran
[d] Department Chemistry, Payame Noor University, P.O. Box, 19395-3697, Tehran, Iran
[e] Department of Chemistry, Gorgan Branch, Islamic Azad University, Gorgan, Iran

ARTICLE INFO

Article history:
Received 1 November 2016
Received in revised form 17 March 2017
Accepted 21 March 2017

Keywords:
Soman
Chlorosoman
BNNT
DFT
Adsorption

ABSTRACT

Adsorption of Soman and Chlorosoman over the outer surface of boron nitride nanotube (BNNT) was studied using density functional theory (DFT) calculations to consider its sensitivity toward mentioned nerve agents. Then, we studied the sensitivity of Ga-doped BNNT and double-antisite defective BNNT (d-BNNT) effects towards adsorbed molecule resulting in eye-catching sensitivity of defected adsorbents representing strong chemical adsorption on the Ga-doped BNNT, while they are mainly physisorbed on the pure BNNT with negligible electronic properties. Density of states (DOSs) was analyzed for further understanding of electronic properties of the applied configurations. Charges were moved from BNNT to the single molecules while in case of Ga-doped and d-BNNT; the charges were transferred from single molecules to the defected adsorbents. These along with outcomes of quantum molecular descriptors, difference in energy gap (E_g), and dipole moments clearly reveal that the d-BNNT is a promising sensor material for the detection of these nerve agents.

1. Introduction

Soman, $C_7H_{16}FO_2P$, also called 3,3-dimethyl-2-butyl methylphospho-noflouridate is belonging to organophosphorus compound and it is an extremely toxic compound. Soman as a chemical nerve agent is colorless liquid with fruity odor. It is recognized as nerve agents owing to their effects over the disruption of nerve impulses in humans which were used in World War I [1–5]. Thus, the adsorption and detection of these chemical nerve agents are very important. In these years, the interaction of the chemical nerve agents including Soman, Sarin, DMMP, Tabun with the different materials have been reported by many researches [6–8]. Recently, scientists have widely explored the usage of BN nanomaterials as polymer composites, gas adsorption, electrical nanoinsulators, electron field emission, and ultraviolet nanoelectronics, and hydrogen-storage [9–17]. In 1994, Rubio et al. have been predicted theoretically boron nitride nanotubes [18], and then experimentally synthesized (arc-discharge method) in 1995 by Chopra and co-workers [19]. BN nanotubes exhibited high thermal conductivity, extraordinary mechanical properties, thermal stability, higher resistance, and higher field emission property. In contrast with the carbon nanotubes, boron nitride nanotubes with a wide energy gap of 5.5 eV, are chemically and thermally more stable. Additional theoretical studies reported BNNT-based gas sensor upon N_2O, CNCl, NH_3, HCOH, and CO molecules or by the BNNTs substituted with atoms such as Al, Ga, and Si [20–24]. For example, the previous reports have been shown that doping functional on the BN nanotubes can be significantly changed the structural, optical, and electronic properties [25–30]. Exclusive properties like high melting point, low density, high thermal conductivity, chemical inertness and wide band gap of a non-oxide ceramic material like Borne Nitride (BN) nanostructures introduce these materials as promising candidate in applications [31,32]. It is an excellent medium for gas sensors, field emission, protective tubular shields, nanotransistors due to its unique mechanical toughness. First born nitride nanotube was fabricated using arc discharge method [33-a]. Its synthesis is mainly nonhelical-type having parallel direction to the tube axis (zigzag configuration).

* Corresponding author at: Golestan Rheumatology Research Center, Golestan University of Medical Science, Gorgan, Iran.
E-mail addresses: Alireza.soltani46@yahoo.com, g.chem1983@gmail.com (A. Soltani).

http://dx.doi.org/10.1016/j.apsusc.2017.03.187
0169-4332/

Different type of defects like, topological defects, transition metal and C doping and B/N vacancies are possible to form as reported [33-b]. Beheshtian et al. reported the surface modification of a boron nitride nanotube (BNNT) with sulfamide molecule has been investigated [34]. Recently, the adsorption of pentachlorophenol (PCP) on the pristine and Fe-doped boron nitride nanotubes was investigated by using density functional theory (DFT) calculations [35]. Their results indicate that the PCP has a weak physisorption on the surface of boron nitride nanotube in comparison with the strong chemisorption on the Fe-doped BNNT. For example, effects of Al doping and double-antisite defect on the adsorption of HCN on a BC_2N nanotube was studied by using density functional theory (DFT) calculations [36]. They have shown that the B-B antisite defect on a BNNT can ameliorate both reactivity and sensitivity of the substrate to hydrogen cyanide. Also CO_2 adsorption on boron antisite (BN) in boron-rich boron nitride nanotube was calculated using PAW-PBE and ONIOM (wB97X-D/6-31G*:AM1) methods [37]. Herein, we investigated the sensing and detecting abilities of the pure, Ga-doped and d-BN nanotubes towards Soman and Chlorosoman molecules.

2. Computational methods

The interactions of Soman and Chlorosoman over the pure, Ga-doped and double-antisite defective BN nanotubes were investigated using DFT calculations. Single-wall zigzag (8, 0) BN nanotube was considered and the (8, 0) SWBNNT containing 56 boron atoms, 56 nitrogen atoms, and 16 hydrogen atoms was selected for this aim. As shown in Table 1, the length of P = O bond in the free Soman and Chlorosoman molecules is about 1.478 and 1.483 Å at B3LYP functional and 1.464 and 1.468 Å at M06-2X functional, respectively. The length and diameter of the BN nanotube are 15.05 and 6.38 Å, respectively, and the average B-N bond length is 1.448 Å (see Fig. 1 and Table 1). The Mulliken charges on B and N atoms in the BN nanotube are 0.619 and −0.619 |e|, showing strong ionicity nature of B-N bonds. The charge of the B defective and Ga doping in the (8, 0) BNNT are about −0.042, and 0.476 e, respectively. In the first step, all the geometrical relaxations and adsorption energies calculations were performed with the aid of Gaussian 03 program package [38] at the level of density functional theory (DFT) at the B3LYP [39,40] functional with 6-311G** standard basis set [41]. In the second step, we have analyzed the interactions of Soman and Chlorosoman on the pure, Ga-doped and defective BN nanotubes in the most stable configurations using M06-2X functional and 6-311G** standard basis set [42]. The B3LYP and M06-2X functionals have been previously reported to study BN nanotubes [43–46]. The basis set superposition error (BSSE) for the adsorption energy was calculated by implementing the counterpoise method [47]. The corresponding adsorption energies (E_{ad}) of the mentioned systems were determined through the following equation:

$$E_a = E_{adsorbent\text{-}adsorbate} - (E_{adsorbent} + E_{adsorbate}) + E_{BSSE} \quad (1)$$

where $E_{adsorbent\text{-}adsorbate}$ is the total energy of Soman and Chlorosoman over applied BN nanotubes. $E_{adsorbate}$ is the total energy of the pure, Ga and B substituted BNNT and $E_{adsorbate}$ is the total energies of Soman and Chlorosoman molecules. The values of highest occupied molecular orbital (HOMO), lowest unoccupied molecular orbital (LUMO), energy difference between the HOMO and the LUMO (E_g), Mulliken population charge analysis (MPA), molecular electrostatic potential (MEP), density of states (DOSs) analyses, and quantum molecular descriptors (QMDs) [48,49] were calculated accordingly at the same level of theory as follows:

$$\mu = -(I + A)/2 \quad (2)$$

$$\chi = -\mu \quad (3)$$

$$\eta = (I - A)/2 \quad (4)$$

$$S = 1/2\eta \quad (5)$$

$$\omega = (\mu^2/2\eta) \quad (6)$$

$$\Delta N_{max} = \frac{-\mu}{\eta} \quad (7)$$

where I ($-E_{HOMO}$) and A ($-E_{LUMO}$) is the energy of the Fermi level and first given value of the conduction band, respectively. Electronegtivity (χ) is defined as the negative of μ, as follows: $\chi = -\mu$. Furthermore, η can be approximated using the Koopmans' theorem [50]. The ω is electrophilicity index and ΔN_{max} represents total amount of charge transfer occurred within a given system [51] (Table 2).

3. Result and discussion

3.1. Adsorption of Soman on BNNT

We firstly investigated whether the BN nanotube can act as an adsorbent for the detection of nerve agents (Soman and Chlorosmoan) over the surface of BN nanotube. For this work, we performed DFT calculations using a hybrid density functional B3LYP method in gas phase. As explored in Fig. 2, the non-covalent interactions between Soman and Chlorosoman with BN nanotubes were occurred at B3LYP functional, as for these complexes the adsorption processes are exothermic in nature. As Table 3 represents the adsorption energy of Soman and Chlorosmoan upon the outer wall of BN nanotube is quite small, around −0.098 eV in form **(a)** and −0.082 eV in form **(b)**, exhibiting a weak physical adsorption over the surface of nanotube owing to Van der Waals forces. Michalkova et al. have similarly reported physisorption of Soman molecule on the edge tetrahedral fragments of clay minerals with an energy value of −0.17 and −0.39 eV at MP2 method and −0.25 eV at HF method [5]. They similarly reported Soman adsorption over Dickiteat different configurations with E_{ad} ranging from −0.17 eV to −0.66 eV using B3LYP and HF methods, respectively [52]. The MPA analysis represents a charge transfer from Chlorosoman to BN nanotube, with the values of 0.044 **(a)** and 0.021e **(b)**. However, the Chlorosoman adsorption upon the outer wall of adsorbent leads to the distances of 2.458 and 2.456 Å (B-N bond) in forms (**a**) and (**b**), respectively. There is a smaller difference between the two kinds of bonds in the BN nanotube. In contrast with Chlorosoman, the adsorption of Soman over BN nanotube had energies about −0.052 **(c)** and −0.049 eV **(d)**. In contrast with the Chlorosoman, it can be seen that the adsorption of Soman give weakest binding with BN nanotube. Our results reveal that Chlorosoman adsorption has low effect on the structural properties. For states **(c)** and **(d)**, the transferred charges from Soman to BN nanotube are calculated just 0.016 and 0.014e, respectively. Our calculation results reveal that the length of C-O bond in the Chlorosoman molecule are altered to 1.484 and 1.483 Å in forms (**a**) and (**b**), while this length bond in an isolated molecule is 1.482 Å. There is only a small hybridization between the BN nanotube forms and those of the Soman molecule, indicating a physisorption process between adsorbate and adsorbent is occurring. In forms **(a)** and **(b)**, about 0.018 and 0.017 electrons are slightly transferred from Soman molecule to BN nanotube, respectively. In contrast with B3LYP functional, the adsorption energy of Soman on the pure BN nanotube is found to be −0.21 eV and the adsorption energy of Chlorosmoan is given by −0.14 eV using M06-2X functional (see Table 4). These are contradictory from the above theoretical values (with the B3LYP functional). Thus, we expect that the pure BN nanotube cannot be served as a sensor for detection of Soman

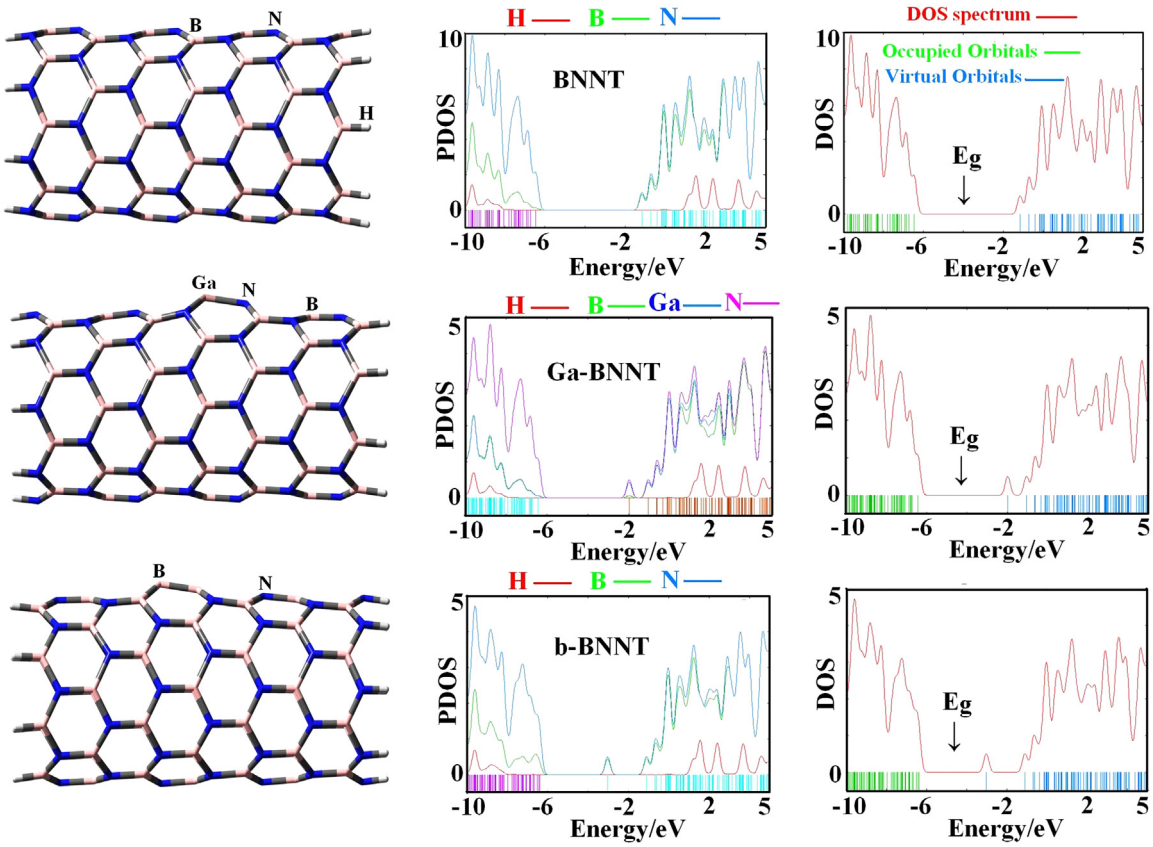

Fig. 1. Adsorption configurations of the pure BNNT, BNGaNT and d-BNNT structures with their corresponding density of state (DOS) plots elaborated in eV.

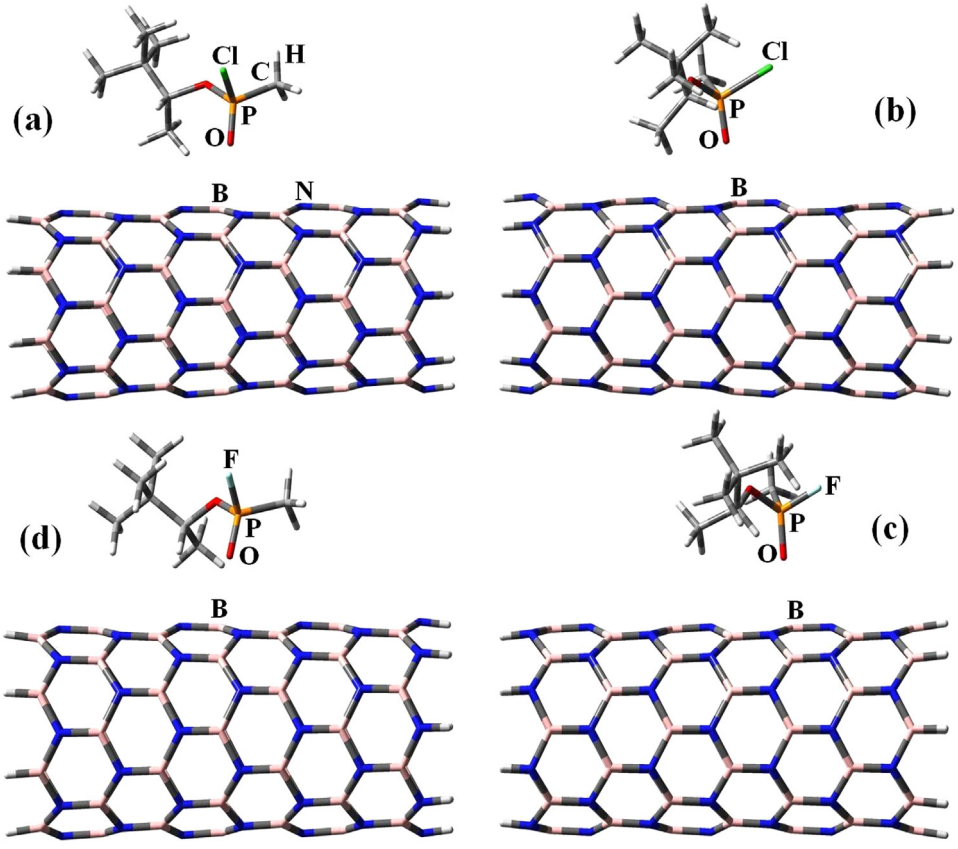

Fig. 2. Adsorption configurations of the Soman and Chlorosoman molecules interacted with the pure BNNT structures.

Table 1
Optimized structural geometries of soman and chlorosoman using the B3LYP and M06-2X functionals. Lengths are in angstrom (Å).

Property	P=O/Å	P—F/Å	P—Cl/Å	P—C/Å	O—C/Å	O=P—O/°	O=P—Cl/°	O=P—F/°
B3LYP								
Smoan	1.478	1.478	–	1.805	1.473	116.9	–	112.5
Chlorosmoan	1.483	–	2.088	1.811	1.474	117.9	111.5	–
M06-2X								
Smoan	1.464	1.591	–	1.785	1.460	116.7	–	111.7
Chlorosmoan	1.468	–	2.066	1.790	1.461	117.0	111.3	–

Table 2
Computed the bond length of the adsorbents, and the adsorbed molecules on the surface of pure, defective, and Ga-doped BN nanotubes.

Property	B—N/Å	Ga—N/Å	B—B/Å	N—B—N	N—Ga—N	B—B—B	P=O/Å	P—F/Å	P—Cl/Å	P—C	O—C/Å
BNNT	1.448	–	–	119.97	–	–	–	–	–	–	–
(a)	1.447	–	–	119.69	–	–	1.479	–	2.095	1.801	1.479
(b)	1.449	–	–	119.65	–	–	1.478	–	2.094	1.802	1.480
(c)	1.448	–	–	119.71	–	–	1.475	1.605	–	1.796	1.479
(d)	1.450	–	–	119.56	–	–	1.475	1.604	–	1.797	1.477
Ga-BNNT	1.447	1.801	–	123.11	113.69	–	–	–	–	–	–
(a)	1.443	1.834	–	123.51	108.02	–	1.507	–	2.047	1.793	1.508
(b)	1.440	1.834	–	123.49	108.16	–	1.502	1.586	–	1.784	1.509
B-BNNT	1.458	–	1.652	124.71	–	115.91	–	–	–	–	–
(c)	1.480	–	1.670	120.62	–	107.55	1.512	–	2.057	1.792	1.497
(d)	1.480	–	1.670	120.62	–	107.70	1.506	1.590	–	1.784	1.500

Table 3
Calculated adsorption energy (Ead/eV), distance (D/ Å), HOMO energies (E_{HOMO}/eV), LUMO energies (E_{LUMO}/eV), HOMO-LUMO energy gap (E_g/eV), Fermi level energy (E_F/eV), and dipole moment (DM/Debye) for all the systems at B3LYP functional.

Property	Ead/eV	D/Å	E_{HOMO}/eV	E_{LUMO}/eV	E_g/eV	ΔE_g/%	E_F/eV	DM/Debye
Smoan	–	–	−7.87	1.60	9.47	–	−3.14	2.968
Chlorosmoan	–	–	−7.84	0.16	8.0	–	−3.84	3.284
BNNT	–	–	−6.45	−1.16	5.29	–	−3.81	11.90
(a)	−0.098	2.842	−6.55	−1.26	5.29	0.0	−3.91	14.25
(b)	−0.082	2.852	−6.52	−1.26	5.26	−0.57	−3.89	12.37
(c)	−0.052	2.779	−6.54	−1.27	5.27	−0.38	−3.91	13.23
(d)	−0.049	2.811	−6.55	−1.23	5.32	−0.57	−3.89	12.42
Ga-BNNT	–	–	−6.43	−1.98	4.45	–	−4.21	12.35
(a)	−1.70	1.987	−6.29	−1.27	5.02	12.81	−3.78	16.56
(b)	−1.48	1.990	−6.28	−1.03	5.25	17.98	−3.66	16.48
B-BNNT	–	–	−6.39	−3.03	3.36	–	−4.71	11.85
(c)	−0.035	1.643	−5.64	−1.37	4.27	27.08	−3.51	14.15
(d)	−0.043	1.652	−5.66	−1.34	4.32	28.57	−3.50	13.79

Table 4
Calculated adsorption energy (Ead/eV), distance (D/Å), HOMO energies (E_{HOMO}/eV), LUMO energies (E_{LUMO}/eV), HOMO-LUMO energy gap (E_g/eV), Fermi level energy (E_F/eV), and dipole moment (DM/Debye) for the most stable configurations at M06-2X method.

Property	Ead/eV	D/Å	E_{HOMO}/eV	E_{LUMO}/eV	E_g/eV	ΔE_g/%	E_F/eV	DM/Debye
Smoan	–	–	−9.91	1.58	11.49	–	−4.17	3.13
Chlorosmoan	–	–	−9.85	1.23	11.08	–	−4.31	3.37
BNNT	–	–	−8.16	−0.39	7.77	–	−4.28	10.70
(a)	−0.14	2.523	−8.04	−0.30	7.74	0.39	−4.17	11.24
(c)	−0.21	2.431	−8.07	−0.33	7.74	0.39	−4.20	11.54
Ga-BNNT	–	–	−8.13	−1.30	6.83	–	−4.72	11.25
(a)	−1.91	1.962	−7.83	−0.08	7.74	13.32	−3.95	15.54
(b)	−1.89	1.964	−7.83	−0.08	7.74	13.32	−3.95	15.63
B-BNNT	–	–	−8.08	−2.31	5.77	–	−5.20	10.75
(c)	−0.75	1.616	−7.02	−0.35	6.67	15.60	−3.69	14.15
(d)	−0.60	1.619	−7.05	−0.37	6.68	15.77	−3.71	13.21

and Chlorosmoan. In the study of the structural properties, the length of B-N bond over the adsorption is changing from 1.448 Å to 1.451 and 1.450 Å in forms **(a)** and **(b)**, respectively, which is in reasonable agreement with the results reported by Zhao and Ding [53]. The value of dipole moment on the interaction of Soman molecule with adsorbent in forms **(a)** and **(b)** are altering from 11.90 Debye in the pristine form to 12.44 and 14.65 Debye, respectively. The inter-atomic bond distances of Soman and Chlorosoman have not experienced noticeable changes though their physisorption over BNNT as we just observed the moderate bond length changes at P-F bonds of Soman molecules through adsorption configurations **(c)** and **(d)** from primary bond length of 1.478–1.605 and 1.604 Å for the mentioned adsorption configurations, respectively. After the weak adsorption occurred at Soman-$[Al(OH)_4]^-$, Soman-$[AlO(OH)_3]^{2-}$, Soman-$[SiO(OH)_3]^-$, and Soman-Si-$(OH)_4$ systems studied by Michalkova et al. [5], the inter-atomic distances of P—F bonds in Soman enlarged about 1.590–1.790 Å from the basic value 1.478 Å reveling a change range of 0.113–0.313 Å and in other work

by the same person the P—F bond length were in the range of 1.596–1.612 Å among fourteen adsorption models at B3LYP and HF methods which is in good agreement with our data of Soman adsorption over pure BNNT with small E_{ad} and difference in the bond length of about 0.13 Å.

As the final stage of study in this section, we studied the orbitals of HOMO and LUMO, and MEP maps of the studied configurations as elaborated in Fig. 3. As it is obvious from the HOMO and LUMO graphs of the studied interactions between Soman and Chlorosoman with BNNT, most of the localizations at both HOMO and LUMO were occurred at the surface of adsorbent with highest contributions of B and N atoms with some partial contribution of ending H atoms. Moreover, low adsorption energy as well as relatively long distances between adsorbent and adsorbate indicates that this interaction is electrostatic in nature [54,55]. The molecular electrostatic potential (MEP) simultaneously represents the size of molecular, shape as well as positive, negative and neutral electrostatic potential areas based on color grading (see Fig. 3). Different electrostatic potential values at the surface of a single molecule or an interaction system distinguished by different colors; red as most negative electrostatic potential region, blue as most positive electrostatic potential region and regions of zero potential have green color. Generally, in case of interaction of Soman and Chlorosoman over the pure BNNT, almost all surface area of these systems represent neutral nature except end regions which blue colored (electropositive or electron poor region) and some reddish region placed between Soman or Chlorosoman and BNNT molecules that stands for the presence and electron rich region generated after the interactions of Soman and Chlorosoman with BNNT. To approve the results of the MEP, we further studied the quantum molecular descriptors (QMDs) presented in Fig. 3, where (χ) is absolute electronegativity (Mulliken electronegativity for atoms) which is constant for an equilibrium complex. The electrons were flowed from lower χ to that of higher χ and moreover it transferred to the lower electronic chemical potential when a Soman and Chlorosoman molecules and BNNT were brought together. Therefore, the χ for pure Soman, Chlorosoman and BNNT were 3.735, 1.843 and 1.858 eV changing to $\geq$2.844 eV for BNNT, while chemical potential for free Soman, Chlorosoman and BNNT were −4.735, −3.840 and −3.805 eV reaching to $\leq$−3.890 eV which represents electron transfer from BNNT to the single adsorbates confirming the above mentioned idea (see Table 3). Considering the Soman and Chlorosoman as **A** and BNNT as **B**, a positive value of ΔN_{max} represents that charge flow occurs from **B** to **A** and the **A** acts as an electron acceptor, while a negative value indicates charge transfer from **A** to **B** and so **A** plays the role of an electron donor. In this regard, the ΔN_{max} for pristine Soman, Chlorosoman and BNNT were 40.8, 26.1 and 39.1 eV which after interaction reached to values $\geq$39.8 eV elaborating the electron flows from BNNT to the single adsorbates as previously reported by Raissi and Mollania [56]. As the obtained results were highly resembled to that of literature reports, we were motivated to suggest some novelty for Soman and Chlorosoman adsorptions to increase their E_{ad} and possible significant changes in electronic properties of the adsorbents which elaborated in the detail in the following sections (Table 5).

3.2. Adsorption of Soman and Chlorosoman Ga-doped BNNTs

Here, after optimization as show in Fig. 4, we studied the adsorption of Soman and Chlorosoman molecules over the geometrical structure and electronic properties of the Ga-doped BN nanotube (Ga-BNNT). We also reported two initial interaction sites for Soman and Chlorosoman molecules. As shown in Fig. 4, structural deformation is created by removing a single B atom with Ga atom in the pure BN nanotube. In a study, the atomic and electronic properties of Ga-BNNT have been calculated using DFT method by Zhukovskii and co-workers. They have shown that the length of Ga—N bond of BN nanotube is 1.80 Å [57]. Our calculations represent that the equilibrium atomic geometries of the nanotube alters after doping process. The length of Ga—N and Ga—N bonds are 1.801 and 1.825 Å, which is larger than the corresponding distance in the same position of the pure BN nanotube of 1.448 and 1.455 Å, which is in reasonable agreement with previous reports [58]. The angle of N—Ga—N and N—Ga—N and Ga—N—B bonds in the pure Ga-BNNT are 113.69 and 114.99°, respectively. There are four kinds of the adsorption states available for Soman and Chlorosoman molecules over the outer surface of Ga-BNNT. The calculations include the chemisorption energy and distance interaction for the complex **(a)** with the value of −1.70 eV is larger than that for the complex **(b)** with the value of −1.48 eV (B3LYP functional) and the corresponding bond lengths of C═O in the complexes **(a)** and **(b)** are 1.513 and 1.514 Å, respectively. On the other hand, we considered the adsorption of Soman and Chlorosoman upon the Ga-BNNT with the contact values of 1.962 **(a)** and 1.964 Å **(b)** and the adsorption energies of −1.91 **(a)** and −1.89 eV **(b)** in the M06-2X functional (see Table 4). We find that the M06-2X functional give the highest adsorption energy in comparison with B3LYP functional. Noticeably, we have seen a decrease and an increase in the bonds of P—C and P═O of Soman and Chlorosoman, respectively, and that is due to the formation of covalent bond of O atoms of Soman and Chlorosoman with Ga atom of Ga-BNNT, that is previously reported by Michalkova et al. when they studied the soman adsorption over $[SiO(OH)_3]^-$ and $[AlO(OH)_3]^{2-}$. Moreover, they reported the same trends for P═O and P—C bond lengths of soman adsorbed over dickite surface [52]. These results appreciably confirm our obtained data. After the adsorption of Soman on the outer wall of adsorbent they have a structure change in the length of Ga—N and Ga—N bonds with an elongated of 1.835 and 1.863 Å in the complex **(a)** and 1.831 and 1.860 Å in the complex **(b)**, respectively. In the previous report [59], we have shown that the adsorption of H_2S on the outer surface of Ga-doped (8, 0) and (5, 5) BN nanotubes and with the gain energy of −1.61 and −1.42 eV, respectively.

Interestingly, as we have shown previously, the Ga doping can appreciably increase the interaction energy of an adsorption system [35,45], as in case of this study, the change of gap energy (ΔE_g) noticeably changed from zero to 12.81% (a) and 17.98% (b), moreover, meaningful results were also observed when we take the dipole moment (DM) of these systems into account, where it significantly altered from 11.90 Debye for bare BNNT to 16.56 and 16.48 Debye for Ga-BNNT producing which are undoubtedly two evidence of sensing ability of Ga-BNNT as it is reported experimentally by Kulkarni and co-workers [60]. The DM of the studied models were 16.56 and 16.48 Debye, which are more than other adsorption systems with is the results of higher adsorption energies of these systems compared to other configurations using pure and d-BNNT adsorbents. Looking at the distribution of charges at HOMO and LUMO states of Soman and Chlorosoman from front view (as presented in Fig. 5) represents that except LUMO for Soman and Chlorosoman interacted with Ga-BNNT, it is mainly placed at right hand side of the presented configuration. Uniform distributions of HOMO and LUMO with more contributions of B and N atoms of Ga-BNNT (Fig. 5) represent low electron transfer after the interaction of Soman and Chlorosoman with Ga-BNNT compared to d-BNNT which stands for the covalent nature of interaction in these four configurations. The MEP plots for both Soman and Chlorosoman interacted with Ga-BNNT are highly resample to each other representing a comprehensive neutral nature of these systems and some electron poor regions at the end of Ga-BNNT and over Soman and Chlorosoman molecules. The QMDs confirms the results of MEP where in case of Soman and Chlorosoman interaction over Ga-BNNT and d-BNNT, both the electronegativity and ΔN_{max} reduced from the basic values representing that Soman and Chlorosoman

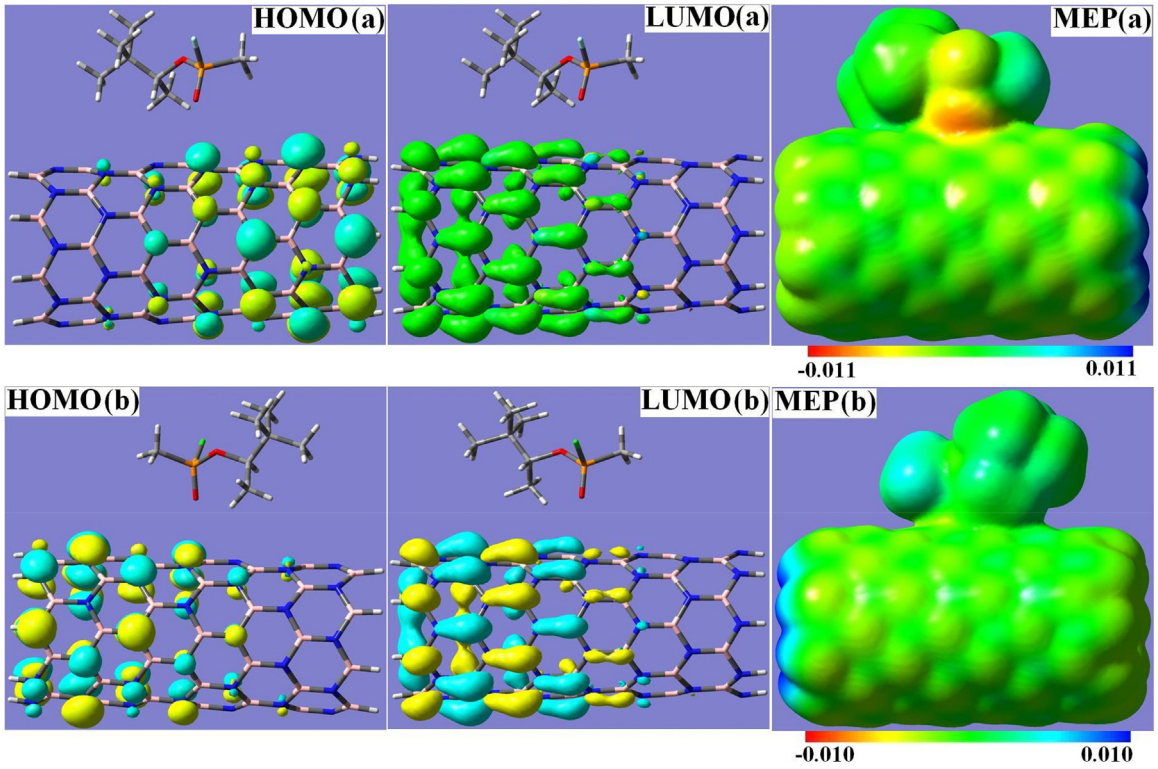

Fig. 3. Frontier molecular orbitals (HOMO & LUMO) and molecular electrostatic maps of the pure BN nanotubes elaborated as yellow or red, blue, and light green colors representing electronegative, electropositive, and neutral regions of the structures. (For interpretation of the references to colour in this figure legend, the reader is referred to the web version of this article.)

Table 5
Calculated quantum molecular descriptors for all the systems mentioned at the B3LYP method.

Property	I/eV	A/eV	η/eV	μ/eV	ω/eV	χ/eV	S/eV	ΔN_{max}/eV
Soman	7.87	−1.60	3.135	−4.735	3.576	4.735	0.106	41.1
Chlorosoman	7.84	−0.16	4.00	−3.840	1.843	3.840	0.125	26.1
BNNT	6.45	1.16	2.645	−3.805	1.858	3.805	0.189	39.1
(a)	6.55	1.26	2.630	−3.890	2.877	3.890	0.190	40.2
(b)	6.52	1.26	2.630	−3.890	2.877	3.890	0.190	40.2
(c)	6.54	1.27	2.635	−3.905	2.893	3.905	0.189	40.3
(d)	6.55	1.23	2.660	−3.890	2.844	3.890	0.188	39.8
Ga-BNNT	6.43	1.98	2.225	−4.205	3.973	4.205	0.225	51.4
(a)	6.29	1.27	2.510	−3.780	2.846	3.780	0.199	40.9
(b)	6.28	1.03	2.625	−3.655	2.544	3.655	0.190	37.9
B-BNNT	6.39	3.03	1.680	−4.710	6.602	4.710	0.297	76.3
(c)	5.64	1.37	2.135	−3.505	2.877	3.505	0.234	44.6
(d)	5.66	1.34	2.160	−3.50	2.835	3.50	0.231	44.1

molecules acts as electron donors based on Raissi and Mollania while the charges of adsorbed molecules increased after interaction [56].

3.3. Adsorption of Soman and Chlorosmoanon the double-antisite defective BNNTs

Thereafter, we investigated the adsorption of Soman and Chlorosoman molecules onto the d-BNNT in order to overcome the low sensitivity of an adsorbent, in which the N atom was replaced by a Ga atom. After substituting the N atom by the B atom, the geometric structure of BN nanotube is dramatically contorted, and two uncommon B—B and B—B bonds were formed. The length of B—B and B—N bonds are found to be 1.652 and 1.458 Å, respectively, which are close to the calculations reported by Choi and co-workers [37]. Thus, the B_1-B_2-B_3 and B_3-N_{II}-B_5 angles in the d-BNNT are calculated to be 117.88 and 116.54°, respectively. We identified the adsorption configurations of Soman and Chlorosoman onto the surface of d-BNNT, as shown in (c) and (d) of Fig. 4. To compare, the physical adsorption energies of Soman and Chlorosoman molecules were slightly altered. The physisorption of Chlorosoman **(c)** and Soman **(d)** onto the surface of d-BNNT are deduced to be −0.035 and −0.043 eV in the B3LYP functional, respectively. The interaction distances between O atom of adsorbate and the boron-rich BN nanotube in configurations **(c)** and **(d)** are 1.638 and 1.646 Å, respectively. In contrast with B3LYP functional, the adsorptions of Chlorosoman **(c)** and Soman **(d)** onto the surface of d-BNNT are found to be −0.75 and −0.60 eV and the distances of 1.616 and 1.619 Å in the M06-2X functional, respectively. Thus, according to the calculations of previous reports [25], these interactions can be considered as an electrostatic interaction.

We found that the adsorptions of Soman and Chlorosoman molecules onto the double-acceptor antisite (B—B bond) BN nanotube are energetically less remarkable than that of the single-acceptor B atom in a BN nanotube. In configurations **(c)** and **(d)**, the length of P═O bond is increased from 1.497 and 1.478 Å in the pure

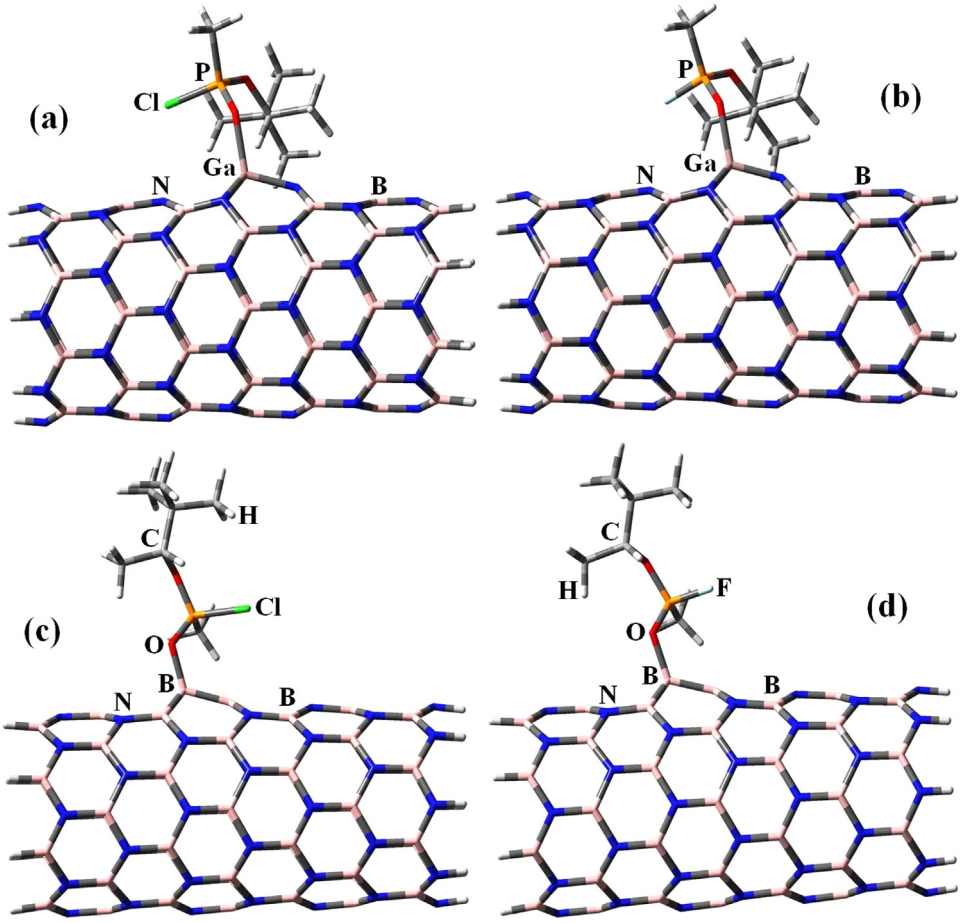

Fig. 4. Adsorption configurations of the Soman and Chlorosoman molecules interacted with Ga-BNNT (a, b) and d-BNNT (c, d) structures.

molecules to 1.518 and 1.514 Å for the adsorption systems, respectively. Rohi et al. [61] reported the lengths of B—B and N—N bonds of BNNT having B_N Stone-Wales Defects are found to be 1.715 and 1.473 Å, respectively, while the B—B bond in our design adsorbate is 1.670 Å. The length of P—Cl and P—F bonds close to the boron-rich BN nano-tubes are slightly abbreviated from 2.097 and 1.600 Å in free form to 2.053 (c) and 1.585 Å (d), respectively. The value of O—P—O bond angle in Soman and Chlorosoman molecules are reduced from 118.24 and 116.94° to 111.95 and 111.82° in configurations **(c)** and **(d)**, respectively. The percentage change in the E_g (ΔE_g) of d-BNNT interacting with Soman molecule through different configurations **(c)** and **(d)** were 27.08 and 28.57% with DM of 14.15 and 13.79 Debye, respectively, representing the high sensitivity of d-BNNT towards Soman and Chlorosoman. Concerning the charge distribution over the presented HOMO-LUMO plots, it is obvious that the main contributions of HOMO and LUMO were allocated to the main bond formed between adsorbent and molecules with some HOMO and LUMO distributions situated at the neighboring atoms of Cl, B and N which along with the highest electron transfer compared to other adsorbents and lower distance between adsorbate and adsorbent indicating reasonable charge transfer for Soman and Chlorosoman adsorbed over d-BNNT which strongly represents a strong electrostatic interaction occurred at these final configurations (see Fig. 5). The MEP plot shows a positive electrostatic potential with blue color and weak negative electrostatic potential, electron rich region with red color, occur at the end (H-capped regions) and main body regions of nanotubes, respectively. This is in good agreement with the outcomes of QMDs where the χ and ΔN_{max} values were experienced some reduction for d-BNNT which is more significant than the adsorption of Soman and Chlorosoman over the pure and Ga-doped BNNTs, representing the B atom in the defective model greater sensitivity to the presence of adsorbate molecules [36]. These results indicate that adsorbed molecules act as electron donor agents.

The density of states (DOSs) spectrum is a useful tool for characterizing the electronic property of a material. The DOS spectrums for the pristine and toxic agents (Soman and Chlorosoman) interacting with the pristine, Ga-BNNT, d-BNNT are shown in Fig. 6. As seen from the spectrums, Soman and Chlorosoman toxic agents with the d-BNNT in comparison to Ga-BNNT found a significant shift of bands to lower energy. However, a significant decrement in the E_g between the conduction band and the valence band upon the adsorption of toxic agents are clearly evident from these spectrums. The attendance of B defective BNNT gives rise to an increase contribution of p-orbitals to their conduction band and the valence band. The DOS spectrum demonstrates that the E_g of B defective BNNT is drastically increased from 3.36 eV to 4.27 and 4.32 eV owing to the adsorption of Soman and Chlorosoman, while the E_g of Ga-BNNT is slightly increased from 4.45 eV to 5.02 and 5.25 eV in Ga-BNNT/Chlorosoman **(a)** and Ga-BNNT/Soman **(b)**, respectively. Therefore, again it the d-BNNT was the most noticeable adsorbent having the lowest E_g standing for the most suitability of this surface for soman and chlorosoman detection. The HOMO energy values in forms Ga-BNNT/Chlorosoman **(a)** and Ga-BNNT/Soman **(b)** are changed to −6.29 and −6.28 eV, whereas this value for the adsorbent is −6.43 eV, respectively. In contrast, the LUMO energy values for the same forms are −1.27 and −1.03 eV, whereas for the pure adsorbents the values are −1.98 eV (see Table 3). The red and blue

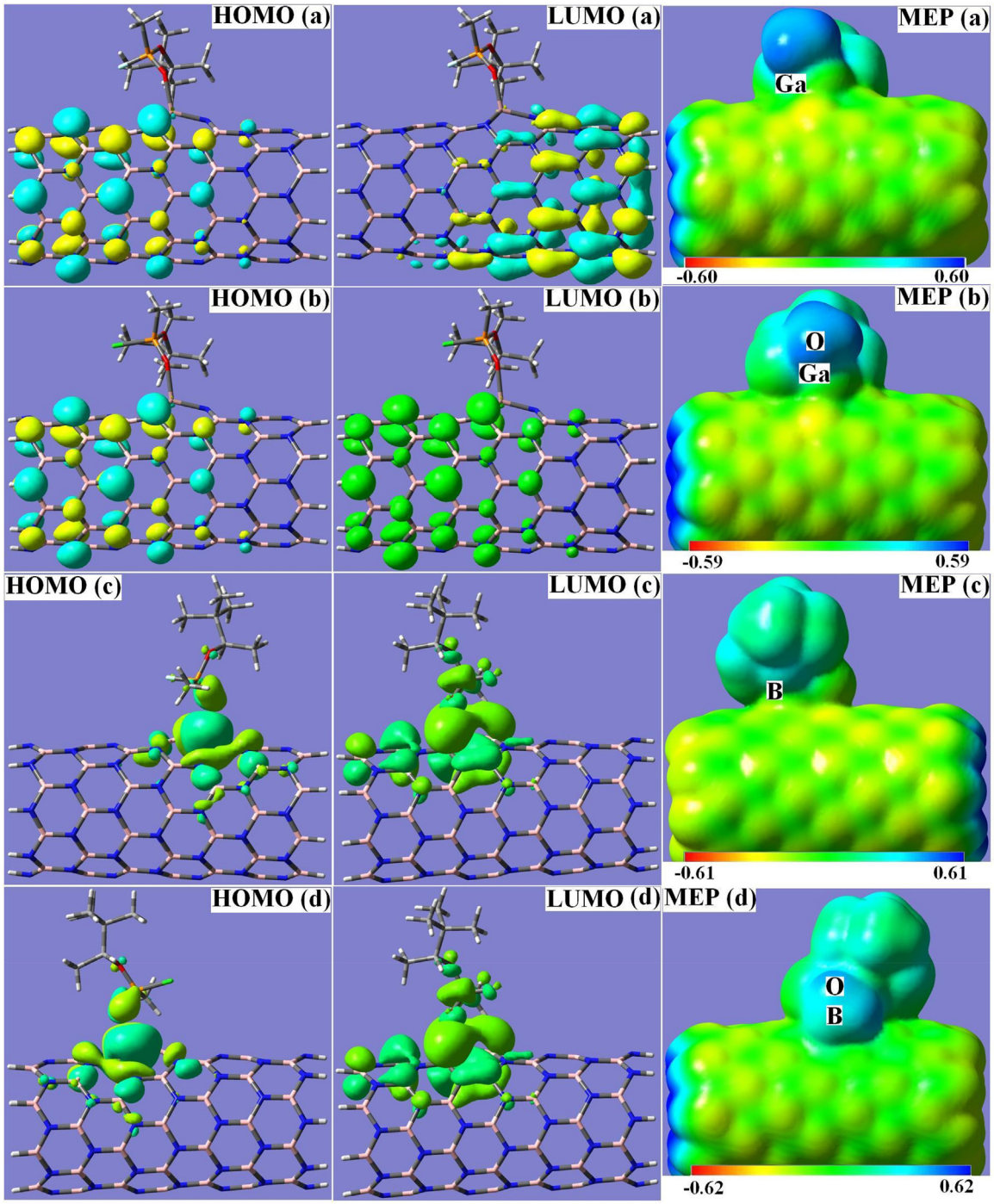

Fig. 5. Frontier molecular orbitals (HOMO & LUMO) and molecular electrostatic maps of the BNGaNT (a, b) and d-BNNT (c, d) structures elaborated as yellow and light green colors representing electronegative, electropositive, neutral regions of the structures. (For interpretation of the references to colour in this figure legend, the reader is referred to the web version of this article.)

colors show the partial population density of states (PDOS) of first (adsorbent) and second (adsorbate) fragments of specified systems. According to the partial density of state presented in the figure we can also seen that the HOMO state of the d-BNNT states for both soman and Cholorosoman interacting molecule is significantly constructed from molecules electronic states unlike other examined systems. Because of chemical adsorption over the gallium states and Soman, peak inside the gap is eliminated. Also in all considered systems, the overlap population density of states (OPDOS) indicates anti-bonding interaction (green color) between adsorbate and adsorbent.

4. Conclusions

We started our studies with the adsorptions of Soman and Chlorosoman over the pure BNNT using B3LYP and M06-2X functionals. As we did not observed noticeable changes within the electronic structure and interaction energy results, we decided to pursue further studies using Ga-BNNT and d-BNNT at the same method, offering us a covalent bond and a non-covalent with noticeable increase in ΔE_g where they were (12.81 and 17.98%) and (27.08 and 28.57%) which were highly significant with the interaction distance of (1.987 and 1.990 Å) and (1.643 and

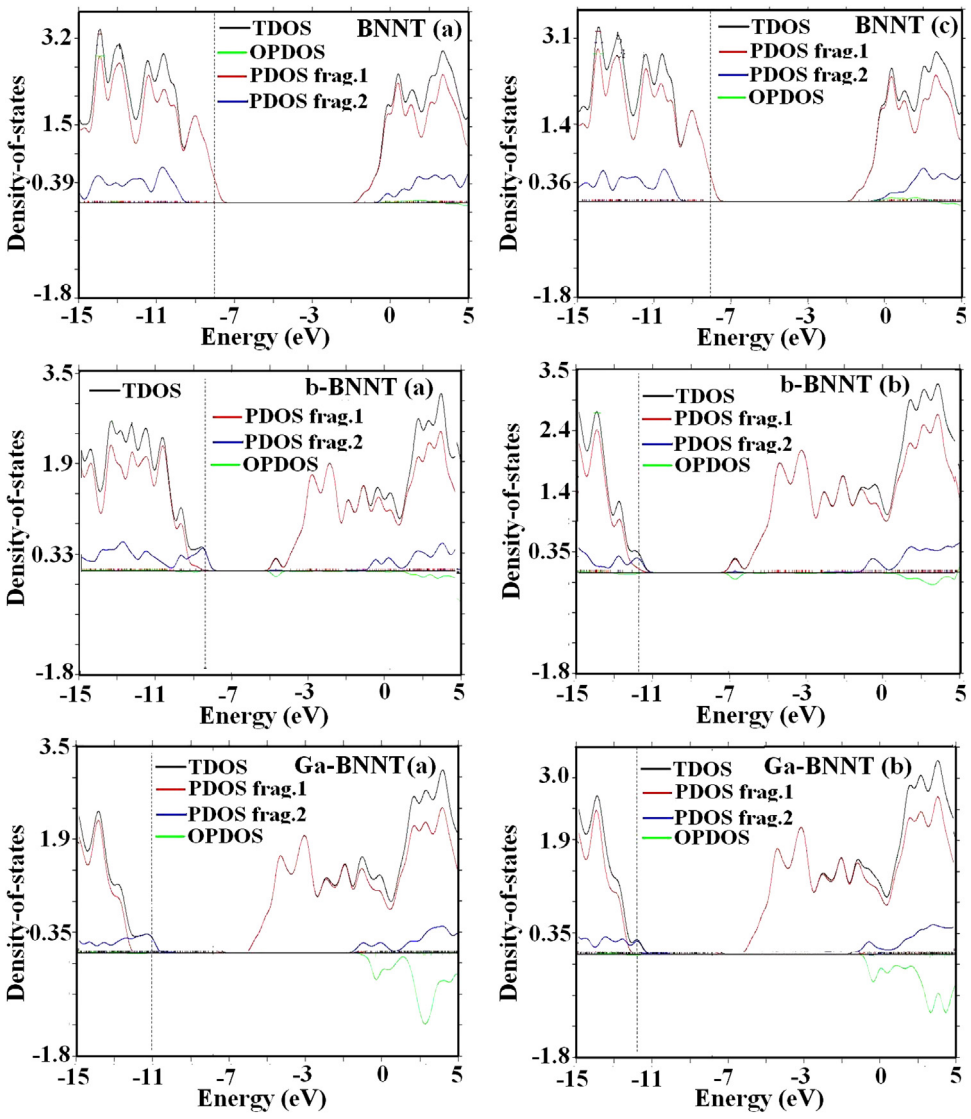

Fig. 6. Parital density of states spectrums for Chlorosoman (left) and Soman (right) interacting with the pristine, d-BNNT and Ga-BNNT nanotubes in most stable configurations indexed with (a), (b) or (c).

1.652 Å) for molecules/Ga-BNNT and molecules/d-BNNT, respectively. The obtained results demonstrate a high sensitivity for d-BNNT compared to the Ga-BNNT on the adsorptions of Soman and Chlorosoman and it may be appropriate sensor for the detection of them.

Acknowledgments

We would like to thank the Nanotechnology Working Group of Young Researchers and Elite Club of Islamic Azad University, Gorgan Branch, Iran. We would like to thank the clinical Research Development Unit (CRDU), Sayad Shirazi Hospital, Golestan University of Medical Sciences, Gorgan, Iran.

References

[1] C. Fest, K.J. Schmidt, The Chemistry of Organophosphorus Pesticides, 352, Springer-Verlag, Berlin, 1982.
[2] A.R.H. Walker, R.D. Suenram, A. Samuels, J. Jensen, M.W. Ellzy, J.M. Lonchner, D. Zeroka, J. Mol. Spectrosc. 297 (2001) 77.
[3] A. Kaczmarek, L. Gorb, A.J. Sadlej, J. Leszczynski, Struct. Chem. 15 (2003) 517.
[4] G. Sarah Sirin, Y. Zhang, J. Phys. Chem. A 118 (2014) 9132–9139.
[5] A. Michalkova, J. Martinez, O.A. Zhikol, L. Gorb, O.V. Shishkin, D. Leszczynska, J. Leszczynski, J. Phys. Chem. B 110 (2006) 21175–21183.
[6] N. Sharma, R. Kakkar, J. Comput. Sci. 10 (2015) 225–236.
[7] A. Michalkova, Y. Paukku, D. Majumdar, J. Leszczynski, Chem. Phys. Lett. 438 (2007) 72–77.
[8] V.M. Bermudez, J. Phys. Chem. C 113 (2009) 1917–1930.
[9] D. Golberg, Y. Bando, C.C. Tang, C.Y. Zhi, Boron nitride nanotubes, Adv. Mater. 19 (2007) 2413–2432.
[10] C.Y. Zhi, Y. Bando, C.C. Tang, S. Honda, K. Sato, H. Kuwahara, D. Golberg, Characteristics of boron nitride nanotube-polyaniline composites, Angew. Chem. Int. Ed. 44 (2005) 7929–7932.
[11] N.G. Chopra, R.J. Luyken, K. Cherrey, V.H. Crespi, M.L. Cohen, S.G. Louie, A. Zettl, Science 269 (1995) 966–967.
[12] A. Loiseau, F. Willaime, N. Demoncy, G. Hug, H. Pascard, Boron nitride nanotubes with reduced numbers of layers synthesized by arc discharge, Phys. Rev. Lett. 76 (1996) 4737–4740.
[13] M. Terrones, W.K. Hsu, H. Terrones, J.P. Zhang, S. Ramos, J.P. Hare, R. Castillo, K. Prassides, A.K. Cheetham, H.W. Kroto, D.R.M. Walton, Metal particle catalysed production of nanoscale BN structures, Chem. Phys. Lett. 259 (1996) 568–573.
[14] W.Q. Han, Y. Bando, K. Kurashima, T. Sato, Appl. Phys. Lett. 73 (1998) 3085–3087.
[15] R.Z. Ma, Y. Bando, H.W. Zhu, T. Sato, C.L. Xu, D.H. Wu, J. Am. Chem. Soc. 124 (2002) 7672–7673.
[16] J.S. Wang, V.K. Kayastha, Y.K. Yap, Z.Y. Fan, J.G. Lu, Z.W. Pan, I.N. Ivanov, A.A. Puretzky, D.B. Geohegan, Nano Lett. 5 (2005) 2528–2532.
[17] Z.G. Chen, J. Zou, Q.F. Liu, C.H. Sun, G. Liu, X.D. Yao, F. Li, B. Wu, X.L. Yuan, T. Sekiguchi, H.M. Cheng, G.Q. Lu, ACS Nano 2 (2008) 1523–1532.
[18] A. Rubio, J.L. Corkill, M.L. Cohen, Phys. Rev. B 49 (1994) 5081.
[19] N.G. Chopra, R.J. Luyken, K. Cherrey, V.H. Crespi, M.L. Cohen, S.G. Louie, et al., Science 269 (1995) 966–967.

[20] M.T. Baei, A.S. Ghasemi, E. Tazikeh Lemeski, A. Soltani, N. Gholami, J. Cluster Sci. 27 (2016) 1081–1096.
[21] A. Soltani, M.T. Baei, A.S. Ghasemi, E. Tazikeh Lemeski, K. Hosseni Amirabadi, Superlattice Microstruct. 75 (2014) 564–575.
[22] A. Soltani, S. Ghafouri Raz, V. Joveini Rezaei, A. Dehno Khalaji, M. Savar, Appl. Surf. Sci. 263 (2012) 619–625.
[23] R. Wang, R. Zhu, D. Zhang, Chem. Phys. Lett. 467 (2008) 131–135.
[24] A. Ahmadi Peyghan, A. Soltani, A.A. Pahlevani, Y. Kanani, S. Khajeh, Appli. Surf. Sci. 270 (2013) 25–32.
[25] A. Soltani, M.T. Baei, E. Tazikeh Lemeski, S. Kaveh, H. Balakheyli, J. Phys. Chem. Solids 86 (2015) 57–64.
[26] J. Wu, W. Zhang, Chem Phys. Lett. 457 (2008) 169–173.
[27] J. Garel, I. Leven, C. Zhi, K.S. Nagapriya, R. Popovitz-Biro, D. Golberg, Y. Bando, O. Hod, E. Joselevich, Nano Lett. 12 (2012) 6347–6352.
[28] Y. Huang, J. Lin, J. Zou, M.-S. Wang, K. Faerstein, C. Tang, Y. Bando, D. Golberg, Nanoscale 5 (2013) 4840–4846.
[29] P. Dev, Y. Xue, P. Zhang, Phys. Rev. Lett. 100 (2008) 117204.
[30] S. Roddaro, A. Fuhrer, P. Brusheim, C. Fasth, H.Q. Xu, L. Samuelson, J. Xiang, C.M. Lieber, Phys. Rev. Lett. 101 (2008) 186802.
[31] P. Shao, X.-Y. Kuang, L.-P. Ding, J. Yang, M.-M. Zhong, Appli. Surf. Sci. 285 (2013) 350–356.
[32] M.D. Ganji, N. Sharifi, A. Fereidoon, M. Ghorbanzadeh Ahangari, Superlattice Microstruct. 67 (2014) 127–143.
[33] (a) R.Z. Ma, D. Golberg, Y. Bando, T. Sasaki, Philos. Trans. R. Soc. Lond. A 362 (2004) 2161;
(b) M. Terrones, M. Romo-Herrera, E. Cruz-Silva, F. Lopez-Urias, E. Munoz-Sandoval, J.J. Velazquez-Salazar, H. Terrones, Y. Bando, D. Golberg, Mater. Today 10 (2007) 40.
[34] J. Beheshtian, A. Ahmadi Peyghan, M. Bigdeli Tabar, Z. Bagheri, Appli. Surf. Sci. 266 (2012) 182–187.
[35] R-x. Wang, D-j. Zhang, R-x. Zhu, C-b. Liu, J. Mol. Model. 20 (2014) 2093.
[36] A. Ahmadi Peyghan, N.L. Hadipour, Z. Bagheri, J. Phys. Chem. C 117 (5) (2013) 2427–2432.
[37] H. Choi, Y.C. Park, Y.-H. Kim, Y.S. Lee, J. Am. Chem. Soc. 133 (2011) 2084–2087.
[38] M. Frisch, G. Trucks, H. Schlegel, G. Scuseria, M. Robb, J. Cheeseman, et al., Gaussian 03, Revision D. 01, Gaussian Inc, Wallingford, CT, 2004.
[39] A.D. Becke, Density-functional thermochemistry. III. The role of exact exchange, J. Chem. Phys. 98 (1993) 5648–5652.
[40] C. Lee, W. Yang, R.G. Parr, Development of the collesalvetti correlation-energy formula into a functional of the electron density, Phys. Rev. B 37 (1988) 785–789.
[41] R. Krishnan, J.S. Binkley, R. Seeger, J.A. Pople, J. Chem. Phys. 72 (1980) 650.
[42] Y. Zhao, D.G. Truhlar, The M06 suite of density functionals for main group thermochemistry, thermochemical kinetics, noncovalent interactions, excited states, and transition elements: two new functionals and systematic testing of four M06-class functionals and 12 other functionals, Theor. Chem. Account 120 (2006) 215–241.
[43] M.T. Baei, M. Ramezani Taghartapeh, E. Tazikeh Lemeski, A. Soltani, Superlattice Microstruct. 72 (2014) 370–382.
[44] A. Soltani, M. Ramezani Taghartapeh, H. Mighani, A.A. Pahlevani, R. Mashkoor, Appl. Surf. Sci. 259 (2012) 637–642.
[45] A. Soltani, M.T. Baei, M. Ramezani Taghartapeh, E. Tazikeh Lemeski, S. Shojaee, Struct. Chem. 26 (2015) 685–693.
[46] A. Soltani, S. Ghafouri Raz, V. Joveini Rezaei, A. Dehno Khalaji, M. Savar, Appli. Surf. Sci. 263 (2012) 619–625.
[47] F. Tournus, J.C. Charlier, Phys. Rev. B 71 (2005) 165421.
[48] N. Saikia, R.C. Deka, Comput. Theor. Chem. 964 (2011) 257–261.
[49] N. Saikia, R.C. Deka, Chem. Phys. Lett. 500 (2010) 65–70.
[50] T. Koopmans, Physica 1 (1933) 104.
[51] J.C. Phillips, Phys. Rev. 123 (1961) 420.
[52] A. Michalkova, L. Gorb, M. Ilchenko, O.A. Zhikol, O.V. Shishkin, J. Leszczynski, J. Phys. Chem. B 104 (2004) 1918–1930.
[53] J-x. Zhao, Y-h. Ding, J. Phys. Chem. C 112 (2008) 20206–20211.
[54] Z.-Y. Deng, J.-M. Zhang, K.-W. Xu, Appli. Surf. Sci. 347 (2015) 485–490.
[55] J. Kaur, P. Singla, N. Goel, Appli. Surf. Sci. 328 (2015) 632–640.
[56] H. Raissi, F. Mollania, Eur. J. Pharm. Sci. 56 (2014) 37–54.
[57] Y.F. Zhukovskii, S. Piskunov, J. Kazerovskis, D.V. Makaev, P.N. D'yachko, J. Phys. Chem. C 117 (2013) 14235–14240.
[58] M.T. Baei, Y. Kanani, V. Joveini Rezaei, A. Soltani, Appli. Surf. Sci. 295 (2014) 18–25.
[59] J-x. Zhao, Y-h. Ding, Diamond Relat. Mater. 19 (2010) 1073–1077.
[60] S. Some, Y. Xu, Y. Kim, Y. Yoon, H. Qin, A. Kulkarni, T. Kim, H. Lee, Sci. Rep. 3 (2013) 1868.
[61] H. Roohi, M. Jahantab, M. Yakta, Struct. Chem. 26 (2015) 11–22.